Lattice dynamics of face-centered-cubic metals using the ionic Morse potential immersed in the sea of free-electron gas

K. Mohammed
Department of Electrical and Computer Engineering, University of California, Santa Barbara, California 93106

M. M. Shukla* and F. Milstein
Department of Mechanical and Environmental Engineering, University of California, Santa Barbara, California 93106

J. L. Merz
Department of Electrical and Computer Engineering, University of California, Santa Barbara, California 93106

(Received 23 May 1983)

Lattice vibrations in six face-centered-cubic metals (i.e., copper, silver, gold, lead, palladium, and nickel) are studied by computing phonon dispersion relations along the principal symmetry directions, and the Debye temperature (Θ_D), the mean-square displacement ($\langle u^2 \rangle$), the effective x-ray characteristic temperature (Θ_m), and the Debye-Waller factor exponent (W), as a function of absolute temperature (T). The model used for the present purpose is the ionic Morse potential immersed in a sea of free-electron gas. This scheme provides a new way to evaluate Morse-function parameters by including the effects of the conduction electrons in the metals. The computed results are found to be in excellent agreement with the available experimental observations for almost all the metals studied.

I. INTRODUCTION

The Morse potential (MP) has been extensively used in the literature for the study of various elastic, mechanical, and thermal properties of crystalline solids. This potential function, as well as others, has been used in the study of defect structures of metals (including stacking faults,[1] dislocations,[2–6] and point defects[7–9]), inert gases in metals,[10,11] equations of state,[12,13] shock-wave propagation in crystals,[14] variation of lattice energy with compression or expansion,[15] elastic properties of metals[13,16] and alloys,[17] lattice distortion at surfaces,[18,19] interactions between gas atoms and crystal surfaces,[20] fracture behavior of metals,[21] and the theoretical strength of ideal crystals.[22,23] The MP expresses the potential energy $\phi(r_i)$ between two atoms separated by a distance r_i as

$$\phi(r_i)=D(e^{-2\alpha(r_i-r_0)}-2e^{-\alpha(r_i-r_0)}) , \tag{1}$$

where D and α are constants with dimensions of energy and (distance)$^{-1}$, respectively. The potential has its minimum at $r_i=r_0$, and the dissociation energy of the two atoms is D since $\phi(r_0)=-D$. There have been several earlier determinations of D, α, and r_0 for cubic metals.[13,16,24,25] To determine the numerical values of these parameters, authors have used a variety of experimental data; for example, Girifalco and Weizer[13] and Lincoln *et al.*[16] used cohesive energy, compressibility, and lattice parameter while Milstein[25] used the experimental values of elastic moduli C_{11}, C_{12}, and the lattice parameter to evaluate the model parameters. It should be pointed out here that all of these authors have discussed the interatomic interactions of metals only by interionic interactions and have ignored the effects of conduction electrons in metals. As a consequence, these authors have either used invariably $C_{12}=C_{44}$, or their theoretical elastic constants predict this equality. In order to overcome this drawback, we have described the case of a metallic atom as being composed of ionic interactions described by MP with the ionic lattice "immersed" into a sea of free-electron gas. We have described the electron interaction by means of a screened Coulomb interaction. There are thus four parameters involved in the present study of metals, namely D, α, r_0, and k_e, the bulk modulus of the electron gas. Since interionic interactions are governed by purely central forces in metals, we immediately have $k_e=C_{12}-C_{44}$. In order to determine the model parameters of MP, we subtracted the electronic part of the elastic constants C_{11}^e and C_{12}^e, given by $C_{11}^e=C_{12}^e=C_{12}-C_{44}$, from the experimental values of the elastic constants C_{11} and C_{12}. This gives the ionic part of the elastic constants C_{11}^i and C_{12}^i, viz.,

$$C_{11}^i=C_{11}-C_{12}+C_{44} , \tag{2}$$

$$C_{12}^i=C_{44}^i=C_{44} . \tag{3}$$

This treatment implicitly assumes that the ionic contribution to the pressure P^i is zero at equilibrium (i.e., where the total pressure is zero). This simplifying approximation is made in order to avoid including the P^i contribution to the ionic moduli C_{ij}^i.[26] The method of determining the Morse parameters [see Eqs. (34)–(36)] ensures that

$P^i=0$ at equilibrium.

By using Eqs. (2) and (3) together with the lattice parameters of the metal and following the scheme of Milstein,[25] we were able to obtain the numerical values of D, α, and r_0 for metals. We have confined our studies to fcc metals only. Equations (2) and (3) show that we have used the ionic part of the elastic constants, which no doubt predict the Cauchy relation. However, when the electronic part of the elastic constants is added, C_{12} and C_{44} are bound to be different and eventually tend to the experimental values.

Our basic aim in this paper is the study of lattice vibrations by using MP in the case of metals; evidently, such a study has not been carried out before. MP was utilized for the study of lattice vibrations in fcc inert-gas solids only by Gupta and Gupta,[27] but such a study is uncomplicated by the presence of conduction electrons either in the determination of the model parameters or in the determination of the phonon spectrum. Gupta and Gupta[27] had arrived at the conclusion that at least 12 nearest-neighbor interactions are needed to reproduce the phonon dispersion curves in inert-gas solids using MP. We were interested in learning how many nearest-neighbor interactions would be required for the case of metals. The interatomic interactions as well as the way of determining the MP parameters is different for inert-gas solids and metals. Thus we found that a study of interionic interactions to the second-nearest neighbor suffices for the determination of phonon dispersion relations in metals. We would like to point out that we tried to study all the fcc metals for which data on elastic constants and phonons were available, but we could study only six: copper, silver, gold, lead, nickel, and palladium, for which the ratio of C_{11}^i and C_{12}^i lies in the limit $1.14<C_{11}^i/C_{12}^i<2.0$; this limitation is discussed further in Sec. V. The phonon dispersion relations along the principal symmetry directions, the Θ_D-T curve, $\langle u^2\rangle$, Θ_M, and the Debye-Waller factor exponent W for all these six metals, form the subject matter of the present study.

II. THEORY

The secular determinant to determine the frequency of vibrations of a solid is given by

$$\det|\underline{D}-m\omega^2\underline{\mathbb{1}}|=0\ , \tag{4}$$

where $\underline{D}$ is the dynamical matrix, m is the ionic mass, ω is the angular phonon frequency, and $\underline{\mathbb{1}}$ is the unit matrix. The dynamical matrix $\underline{D}$ is split into two parts: the ionic part $\underline{D}^i$ which is based on MP and the electronic part $\underline{D}^e$ which is based on the model of Krebs,[28]

$$D_{\alpha\beta}=D^i_{\alpha\beta}+D^e_{\alpha\beta}\ . \tag{5}$$

By confining the interionic interactions to the second-nearest neighbors only, the typical diagonal and nondiagonal parts of the ionic dynamical matrix elements are given by

$$D^i_{\alpha\alpha}=2(\phi_1''+\phi_1')[2-C_i(C_j+C_k)]+4\phi_1'(1-C_jC_k)+4\phi_2''(1-C_i^2)+\phi_2'[2-(C_j^2+C_k^2)]\ , \tag{6}$$

$$D^i_{\alpha\beta}=2(\phi_1''-\phi_1')S_iS_j\ . \tag{7}$$

In the above equations, $C_i=\cos(\pi ak_i)$, $S_i=\sin(\pi ak_i)$, a is the lattice parameter, and k_i is the ith component of the phonon wave vector. ϕ_i' is the first derivative of ith-neighbor Morse function divided by the ith-neighbor distance and ϕ_i'' is the second derivative of the ith-neighbor Morse function. The electronic part of the dynamical matrix elements is given by

$$D^e_{\alpha\alpha}=\tfrac{1}{4}a^3\lambda^2k_e\sum_h\left[\frac{(q_i+h_i)^2g^2(u_1)}{|\vec{q}+\vec{h}|^2+(a^2\lambda^2/4\pi^2)f(t_1)}-\frac{h_i^2g^2(u_2)}{h^2+(a^2\lambda^2/4\pi^2)f(t_2)}\right]\ , \tag{8}$$

$$D^e_{\alpha\beta}=\tfrac{1}{4}a^3\lambda^2k_e\sum_h\left[\frac{(q_i+h_i)(q_j+h_j)g^2(u_1)}{|\vec{q}+\vec{h}|^2+(a^2\lambda^2/4\pi^2)f(t_1)}-\frac{h_ih_jg^2(u_2)}{h^2+(a^2\lambda^2/4\pi^2)f(t_2)}\right]\ , \tag{9}$$

$$k_e=C_{12}-C_{44}\ , \tag{10}$$

$$\lambda=0.353(r_s/a_0)^{1/2}k_F\ , \tag{11}$$

$$g(u)=\frac{3}{u^3}(\sin u-u\cos u)\ , \tag{12}$$

$$f(t)=\tfrac{1}{2}+\frac{1-t^2}{4t}\ln\left|\frac{1+t}{1-t}\right|\ , \tag{13}$$

$$k_F=(9\pi/4)^{1/3}\frac{1}{r_s}\ , \tag{14}$$

$$r_s=(3/4\pi n_e)^{1/3}\ , \tag{15}$$

$$u_1=\frac{2\pi r_s}{a}|\vec{q}+\vec{h}|\ , \tag{16}$$

$$u_2=\frac{2\pi r_s}{a}\,|\vec{h}|\ , \tag{17}$$

$$t_1=\frac{\pi\,|\vec{q}+\vec{h}|}{ak_F}\ , \tag{18}$$

$$t_2=\frac{\pi\,|\vec{h}|}{ak_F}\ . \tag{19}$$

In the above equation, a_0 is the Bohr radius, $q_i=ak_i/2\pi$, and h_i $(i=1,2,3)$ represent the Cartesian components of the reciprocal-lattice vector. The phonon dispersion relations in the principal symmetry directions are given by simple analytical functions of the form

$$m\omega^2_{\mathrm{L}(q,0,0)}=4(\phi_1''+\phi_1')(1-C_i)+4\phi_2''(1-C_i^2)+[D^e(q,0,0)]_{11}\ , \tag{20}$$

$$m\omega^2_{\mathrm{T}(q,0,0)}=2(\phi_1''+\phi_1')(1-C_i)+4\phi_2'(1-C_i^2)+[D^e(q,0,0)]_{33}\ , \tag{21}$$

$$m\omega^2_{\mathrm{L}(q,q,q)}=(4\phi_1''+4\phi_2''+\phi_1'+2\phi_2')(1-C_i^2)+[D^e(q,q,q)]_{11}+2[D^e(q,q,q)]_{12}\ , \tag{22}$$

$$m\omega^2_{\mathrm{T}(q,q,q)}=(4\phi_1''+\phi_1'+4\phi_2''+2\phi_2')(1-C_i^2)+[D^e(q,q,q)]_{11}-[D^e(q,q,q)]_{12}\ , \tag{23}$$

$$m\omega^2_{\mathrm{L}(q,q,0)}=2(\phi_1''+\phi_1')[2-C_i(C_i+1)]+[4\phi_1'+(4\phi_2''+\phi_2')(1+C_i)](1-C_i)$$
$$+2(\phi_1''+\phi_1')S_i^2+[D^e(q,q,0)]_{11}+[D^e(q,q,0)]_{12}\ , \tag{24}$$

$$m\omega^2_{\mathrm{T}(q,q,0)}=2(\phi_1''+\phi_1')[2-C_i(C_i+1)]+[4\phi_1'+(4\phi_2''+\phi_2')(1-C_i)](1-C_i)$$
$$-2(\phi_1''+\phi_1')S_i^2+[D^e(q,q,0)]_{11}-[D^e(q,q,0)]_{12}\ , \tag{25}$$

$$m\omega^2_{\mathrm{T}_2(q,q,0)}=4(\phi_1''+\phi_1')(1-C_i)+2(2\phi_1'+\phi_2')(1-C_i^2)+[D^e(q,q,0)]_{33}\ , \tag{26}$$

$$m\omega^2_{\mathrm{L}(1,q,0)}=2(\phi_1''+\phi_1')(3+C_i)+[4\phi_1'+\phi_2'(1+C_i)](1-C_i)+[D^e(1,q,0)]_{11}+[D^e(1,q,0)]_{12}\ , \tag{27}$$

$$m\omega^2_{\mathrm{T}_1(1,q,0)}=2(\phi_1''+\phi_1')(3+C_i)+[4\phi_1'+\phi_2'(1+C_i)](1-C_i)+[D^e(1,q,0)]_{11}-[D^e(1,q,0)]_{12}\ , \tag{28}$$

$$m\omega^2_{\mathrm{T}_2(1,q,0)}=2(\phi_1''+\phi_1')(1-C_i)+[4\phi_1'+\phi_2'(1-C_i)](1+C_i)+[D^e(1,q,0)]_{33}\ . \tag{29}$$

The usual thermal properties of crystals, i.e., lattice heat capacity C_V, Debye temperature Θ_D, the effective x-ray characteristic temperature Θ_M, Debye-Waller factor exponent W, and mean-square displacement $\langle u^2\rangle$, are calculated through the following expressions:

$$C_V=k_B\int_0^{\nu_{\max}}\frac{(h\nu/k_BT)^2\exp(h\nu/k_BT)}{[\exp(h\nu/k_BT)-1]^2}g(\nu)d\nu\ , \tag{30}$$

$$W=\frac{4\pi^2\hbar}{3mN}(\sin\theta/\lambda)^2\sum_{qj}\frac{1}{\omega_{qj}}\coth\frac{\hbar\omega_{qj}}{2k_BT}\ , \tag{31}$$

$$\Theta_M^2=\frac{6\hbar^2T}{mk_BW}[\phi(x)+(x/4)](\sin\theta/\lambda)^2\ , \tag{32}$$

$$\langle u^2\rangle=\frac{3}{8\pi^2}(\lambda/\sin\theta)^2W\ . \tag{33}$$

In the above expressions, $\phi(x)$ is the usual Debye integral function and $x=\Theta_M/T$, N is the total number of unit cells in the crystal, q_j is the jth component of the phonon wave vector, ω_{qj} is the angular frequency for the q_j mode, λ is the wavelength of the incident radiation, and θ is the glancing angle of incidence.

III. NUMERICAL COMPUTATIONS

The numerical computations consist of two parts: the determination of the model parameters of the MP for the metals, and evaluation of phonon spectra and thermal properties of metals. In order to evaluate the model parameters, we have used three different equations following the scheme of Milstein,[25]

$$C^i_{11}=C_{11}-C_{12}+C_{44}=\frac{n}{32a^3}[PG(2\alpha a)-QG(\alpha a)]\ , \tag{34}$$

$$C^i_{12}=C_{44}=\frac{n}{32a^3}[PH(2\alpha a)-QH(\alpha a)]\ , \tag{35}$$

$$PF(2\alpha a)=QF(\alpha a)\ , \tag{36}$$

where the symbols P, Q, $G(\alpha a)$, $H(\alpha)$, and $F(\alpha a)$ are functions of the parameters D, α, and r_0 (see Ref. 25 for more details). The input data, i.e., the elastic constants and the lattice parameters to determine D, α, and r_0, are given in Table I, along with the numerical values of these parameters. With a knowledge of α, D, r_0, and k_e we calculated the phonon dispersion relations for all of the six metals listed in Table I along the principal symmetry directions: $[q00]$, $[qq0]$, $[qqq]$, and $[1q0]$.

The dispersion curves for copper, silver, gold, nickel, lead, and palladium are given in Figs. 1—6, together with the corresponding experimental points for comparison. In order to determine the phonon density of states for all six metals, we have solved the secular determinant for a discrete subdivision of the wave-vector space. The first Brillouin zone was thus divided into an evenly spaced

TABLE I. Values of elastic constants C_{11}^i and C_{12}^i, lattice parameter a, and Morse-function parameters D, α, and r_0 for fcc crystal lattice.

Metal	C_{11}^i (10^{11} dyn/cm^2)	C_{12}^i (10^{11}dyn/cm^2)	a (Å)	D (10^{-13} erg)	α (Å^{-1})	r_0 (Å)
Ni	19.660	12.200	3.52	3.6927	2.0198	2.5736
Cu	12.140	7.540	3.61	2.4047	2.0102	2.6328
Ag	7.670	4.610	4.08	1.9514	1.9067	2.9536
Pd	12.270	7.170	3.89	2.3604	2.1719	2.7970
Pb	2.750	1.819	4.95	1.8294	1.2022	3.7292
Au	7.19	4.27	4.07	1.7163	1.9788	2.9372

sample of 8000 wave vectors. Crystal symmetry permitted us to solve for only 262 nonequivalent wave vectors including the origin. The width of frequency was taken to be $\Delta\nu=0.05\times10^{12}$ sec^{-1} to plot $g(\nu)$-vs-ν curves. The specific heat at constant volume was calculated from a knowledge of the $g(\nu)$-vs-ν curve and using Eq. (30). The corresponding Θ_D-T curves for all the six metals are shown in Figs. 7–12, together with the experimental points for comparison. The entire phonon spectra were utilized to compute x-ray characteristic temperature Θ_M, mean-square displacement of atoms $\langle u^2\rangle$, and the Debye-Waller factor exponent W.

IV. COMPARISON WITH EXPERIMENTAL RESULTS

A. Copper

The experimental phonon dispersion curves of copper have been determined by various workers. The most reliable results are those of Svensson *et al.*[29] We have compared our theoretical results with their data. Figure 1 shows that the calculated dispersion curves have almost reproduced the experimental frequencies. A small divergence of about 2–4 % between the computed and experimental phonons is noted in $[q00]_L$, $[qq0]_{T_2}$, and $[qqq]_T$ for certain wave vectors in the high-frequency region. From Fig. 7 we see the calculated Θ_D-T curve for copper has reproduced the entire shape of the experimental curve but it lies about 2% lower than the experimental points. The reason behind this is very simple: In order to calculate the Θ_D-T curve we have used the $g(\nu)$-vs-ν curve for room temperature instead of that for $T=0$ K. The experimental values of Θ_D have been taken from Martin.[30] The comparison of calculated and experimental values of Debye-Waller factors is made in terms of the Debye-Waller–temperature parameter only, defined by

$$Y=(\lambda/\sin\theta)^2(2W_{T_0}-2W_T)\log_{10}e\ , \tag{37}$$

where $2W_T$ and $2W_{T_0}$ are the values of Debye-Waller factors at temperatures T and T_0. This quantity is independent of λ and θ. Figure 13 shows that there is an excellent agreement between the calculated and experimental values of Y, $\langle u^2\rangle$, and Θ_M of copper below 300 K. Above that, theoretical results show some disagreement with the experiment. The experimental values of W, Θ_M, and $\langle u^2\rangle$ for copper have been taken from the works of Owen and Williams,[31] Flinn *et al.*,[32] and Chipman and Paskini.[33]

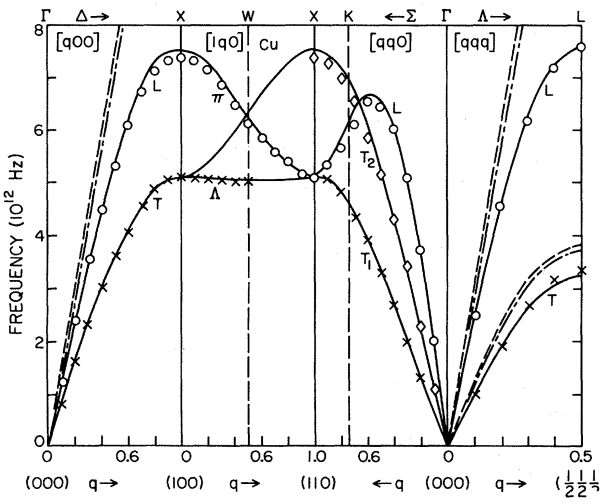

FIG. 1. Dispersion curves for copper along the $[q00]$, $[1q0]$, $[qq0]$, and $[qqq]$ directions. Experimental data of Svensson *et al.* (Ref. 29) are shown by circles, squares, and dots. Solid lines show the theoretical fits by the present study. Dashed and dotted-dashed lines indicate the computed fits using D, α, and r_0 determined by Milstein (Ref. 25) and Girifalco and Weizer (Ref. 13).

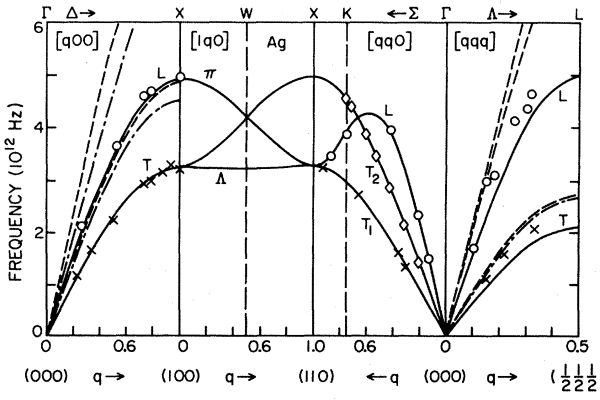

FIG. 2. Dispersion curves for silver. Experimental data are from Kamitakahara and Brockhouse (Ref. 35). Other details given in caption of Fig. 1.

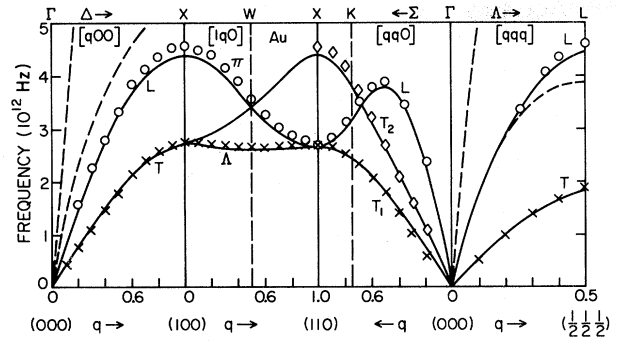

FIG. 3. Disperson curves for gold. Experimental data are from Lynn *et al.* (Ref. 42). Other details given in caption of Fig. 1. MP's were not available from Girifalco and Weizer.

B. Silver

Drexel *et al.*[34] and Kamitakahara and Brockhouse[35] have measured the phonon dispersion relations in silver. We have compared our theoretical calculations with the results of Kamitakahara and Brockhouse;[35] these results are more detailed than those of Drexel *et al.* From Fig. 2 we note that the theoretical dispersion curves have almost reproduced the experimental results for the directions $[q00]$ and $[qq0]$. A small divergence is noted between the calculated and experimental phonons in the $[qqq]$ direction. If we take account of the experimental uncertainties in the measured phonons, the maximum deviation between the calculated and observed frequency in $[qqq]$ does not exceed 5%. Figure 9 shows that the calculated Θ_D-T curve of silver has the correct shape of the experimental curve and lies about 2% below the experimental curve. The experimental values of Θ_D were taken from the measurements of Meads *et al.*[36] In order to estimate the observed specific heat we have taken $\gamma=0.65$ mJ mol^{-1}deg^{-2} from the work of Hoare and Yates.[37] Figure 14 reveals that the calculated Y, Θ_M, and $\langle u^2\rangle$ of silver are in excellent agreement with the experimental results below 200 K. The experimental values of Y, Θ_M, and $\langle u^2\rangle$ have been taken from the measurements of

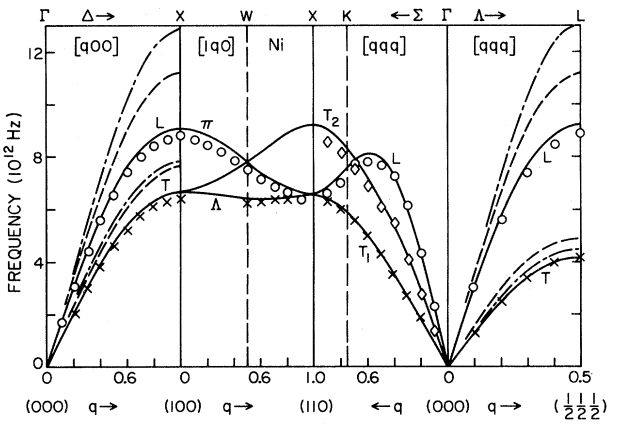

FIG. 4. Dispersion curves for nickel. Experimental data are from Birgeneau *et al.* (Ref. 48). Other details given in caption of Fig. 1.

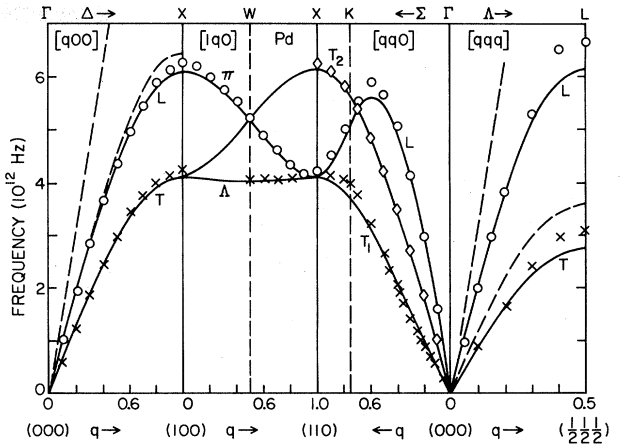

FIG. 5. Dispersion curves for palladium. Experimental data are from Miller and Brockhouse (Ref. 51). Other details given in caption of Fig. 1. MP's were not available from Girifalco and Weizer (Ref. 13).

Boskovits *et al.*,[38] Andriessen,[39] Spreadborough and Christian,[40] and Simareká.[41]

C. Gold

The experimental phonon frequencies in gold were measured by Lynn *et al.*[42] A study of Fig. 3 shows that the computed phonon dispersion relations in gold have almost reproduced the experimental curves along all the symmetry directions. The computed phonons show a maximum departure of about 5% from the experimental phonons in the high-frequency region, and that along $[qqq]_L$, $[q00]_L$, and $[qq0]_L$ only. Figure 9 shows that the experimental Θ_D-T curve of gold has almost been reproduced by the theoretical curve. The calculated and experimental Θ_D differ at the most by only 2%. In order to estimate the experimental Θ_D from C_V, we have subtracted the electronic part of the specific heat γ, given by $\gamma=177.6\times10^{-6}$ cal deg^{-2} g-at^{-1}, taken from the experimental measurements of Corek *et al.*[43] The experimental values of C_V below 30 K were taken from the work of Martin,[44] and above 30 K from those of Geballe and Giauque.[45] From Fig. 15 we see that the computed Y and $\langle u^2\rangle$ give an excellent account of the experimental curves.

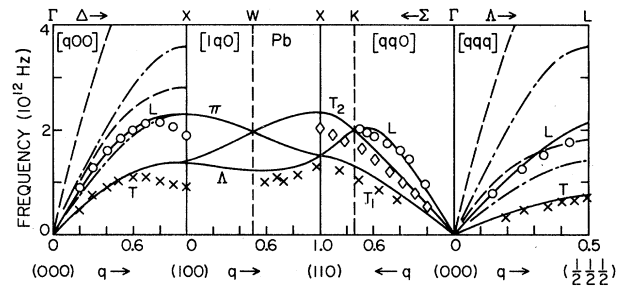

FIG. 6. Dispersion curves for lead. Experimental data are from Brockhouse *et al.* (Ref. 54). Other details given in caption of Fig. 1.

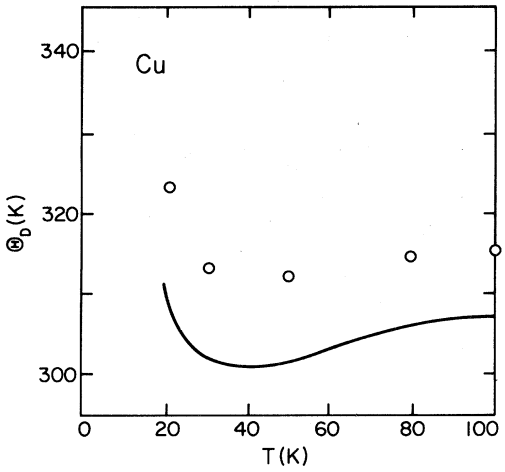

FIG. 7. Θ_D-T curves for copper. Experimental data from Ref. 30 are marked by open circles. Solid lines are calculated fits.

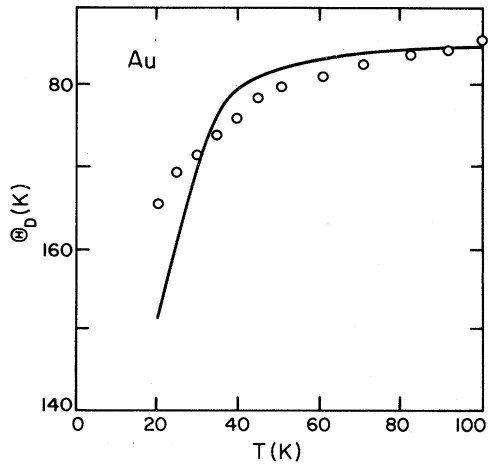

FIG. 9. Θ_D-T curves for gold. Experimental data are taken from Ref. 44 for values measured below 30 K and from Ref. 45 for values above that. Other details given in caption of Fig. 7.

However, the computed Θ_M does not give as good a description of the experimental curve. While $\langle u^2 \rangle$ still gives satisfactory results for experiments below 900 K, Y departs significantly above 700 K. The experimental values of Y, Θ_M, and $\langle u^2 \rangle$ were taken from the work of Owen and Williams.[31]

D. Nickel

Phonon dispersion relations in nickel have been measured by Tuberfield,[46] Stringfellow and Torrie,[47] and most extensively by Birgeneau *et al.*[48] whose data are compared here with our calculations. A study of Fig. 4 shows that the calculated phonon dispersion relations have almost reproduced the experimental ones in all symmetry directions. Some departure is noted between the calculated and experimental phonons, of the order of 5% in the high-frequency region, and again in the $[q00]_L$, $[qq0]_L$, and $[qqq]_L$ directions.

Figure 10 shows that the computed Θ_D-T curve for nickel gives a good description of the experimental curve, but lies about 2% below it. We have used the experimental Θ_D from the work of Busey and Giauque.[49] Since nickel is ferromagnetic below 631 K, there is also a spin-wave contribution to the lattice specific heat in addition to the usual electronic contribution. In order to calculate the lattice specific heat, these two contributions have to be subtracted from the heat-capacity data. The electronic heat-capacity coefficient γ was taken to be $\gamma = 7.05 \times 10^{-3}$ J mol^{-1} deg^{-2}, and the spin-wave contribution coefficient C_m was taken to be $C_m = 8.8 \times 10^{-5}\, T^{3/2}$ mol^{-1} deg$^{-3/2}$. From Fig. 16 we see that the calculated Y is in reasonable agreement with experimental results up to 600 K. The calculated Θ_M and $\langle u^2 \rangle$ show reasonable agreement with the experimental data only up to 400 K. The experimental values of Y, Θ_M, and $\langle u^2 \rangle$ are from the measurements of Simareká[41] and Wilson *et al.*[50]

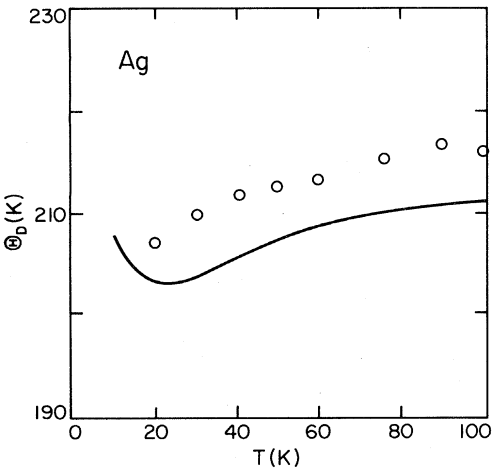

FIG. 8. Θ_D-T curves for silver. Experimental data from Ref. 36. Other details given in caption of Fig. 7.

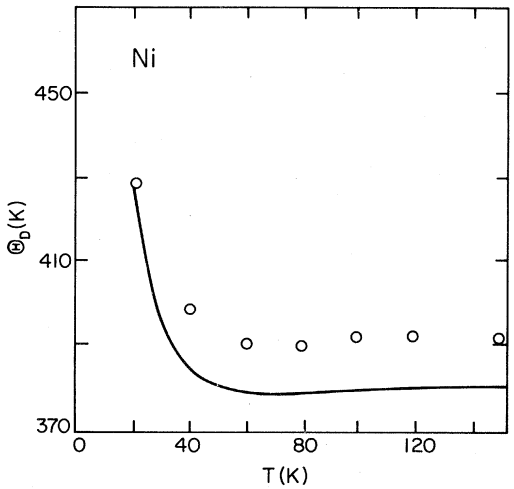

FIG. 10. Θ_D-T curves for nickel. Experimental data are Ref. 51. Other details given in caption of Fig. 7.

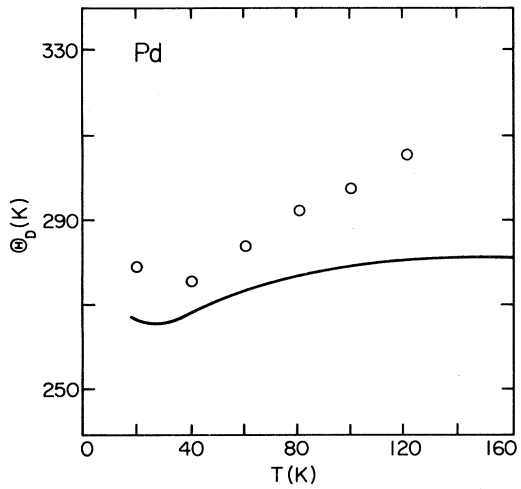

FIG. 11. Θ_D-T curves for palladium. Experimental data below 80 K are from Ref. 52 and data above that are from Ref. 53. Other details given in caption of Fig. 7.

E. Palladium

The phonons in palladium were measured by Miller and Brockhouse.[51] They have provided such measurements at four different temperatures but for the present study we utilized the room-temperature data. A study of Fig. 5 shows that the theoretical phonon dispersion curves have almost reproduced the experimental curves in almost all the symmetry directions and at low and middle q values. There are slight differences between the calculated and experimental phonon in $[qqq]_T$ and $[qq0]_L$ but in no case, however, is the theoretical phonon frequency found to be more than 5% higher or lower than the experimental one. Figure 11 shows that the theoretical Θ_D-T curve of palladium gives a fair description of the experimental curve. While the theoretical curve predicts almost a constant value of Θ_D at higher temperatures, experimental Θ_D still rises further. The experimental value of C_v for palladium was taken from the work of Pickard and Simon[52] below 80 K and that of Clusius and Schachinger[53] above 80 K. The observed values of lattice heat capacities were taken after subtracting the electronic heat-capacity part; for this purpose the coefficient γ was taken to be 13.0 J mol^{-1} deg^{-2}. For palladium we have not calculated the theoretical results for Y, $\langle u^2 \rangle$, and Θ_M since there are no experimental results available.

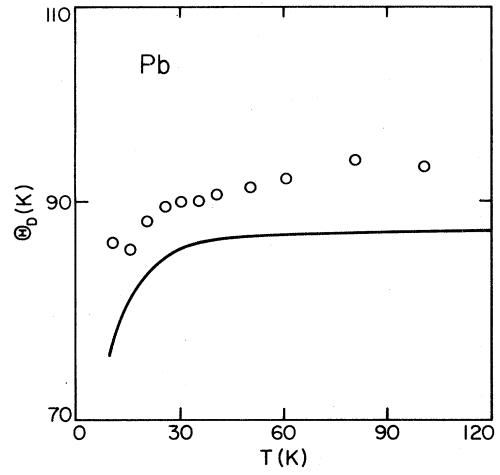

FIG. 12. Θ_D-T curves for lead. Experimental data for C_V below 15 K are from Ref. 57 and data above that are from Ref. 58. Other details given in caption of Fig. 7.

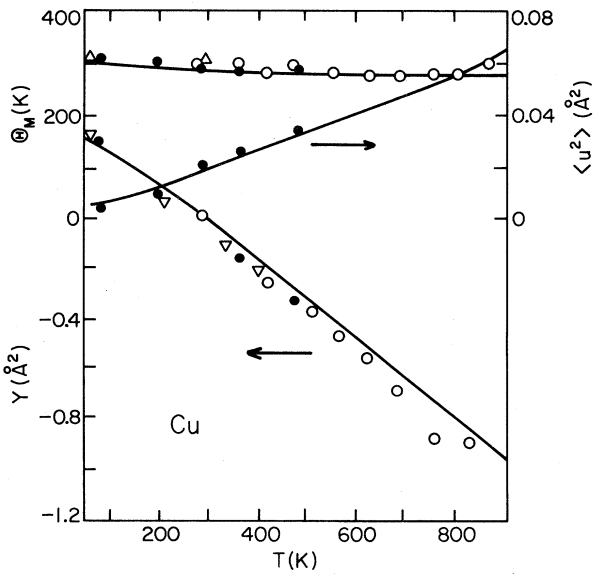

FIG. 13. Temperature variation of y, Θ_M, and $\langle u^2 \rangle$ for copper. Solid lines show the present result. Experimental points: solid circles from Ref. 32, open circles from Ref. 31, and triangles from Ref. 33.

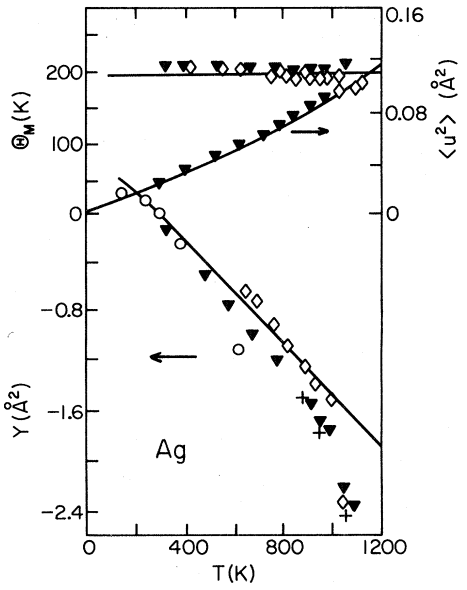

FIG. 14. Temperature variation of y, Θ_M, and $\langle u^2 \rangle$ for silver. Solid lines are for the present result. Experimental points: open circles from Ref. 38, closed squares from Ref. 39, crosses from Ref. 40, and triangles from Ref. 41.

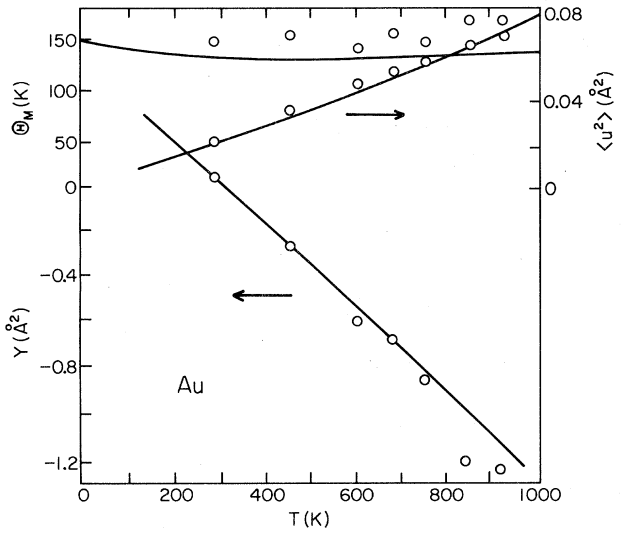

FIG. 15. Temperature variation of y, Θ_M, and $\langle u^2\rangle$ for gold. Solid lines show the present result. Experimental points (open circles) are from Ref. 31.

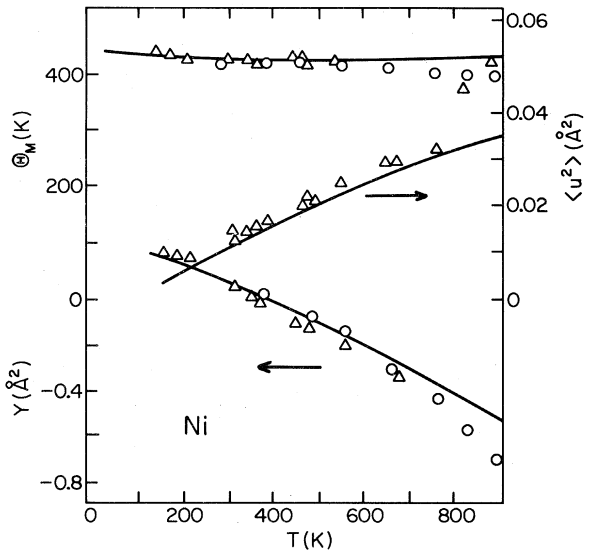

FIG. 16. Temperature variation of y, Θ_M, and $\langle u^2\rangle$ for nickel. Solid lines show the present calculations. Experimental points: open circles are from Ref. 41 and triangles from Ref. 50.

F. Lead

It is evident from Fig. 6 that theoretical calculations reproduce experimental data reasonably well along all the principal symmetry directions. The experimental dispersion curves, obtained by Brockhouse *et al.*,[54] exhibit Kohn anomalies which are not reproduced by the theoretical curves. Except in the region of Kohn anomalies, where the departure between the two curves amounts to 13%, the maximum departure between the calculated and experimental frequencies is not more than 10%. It is also clear from Fig. 12 that the computed Θ_D-T curve is able to predict the correct shape of the experimental curve. The theoretical curve lies approximately 5% below the experimental curves. The deviations of the calculated values of Θ_D from the experimental ones increase with the increase of temperature; at about 70 K, this amounts to about 8%. While the theoretical curve attains saturation above 90 K, the experimental curve shows a trend to rise up further. This kind of result is a bit peculiar and would probably be due to anharmonic effects, strong electron-phonon interactions, or spin-orbit coupling in lead. The experimental values of C_v below 15 K were taken from the work of Van der Hoeven and Keesom,[55] and that above 15 K from the work of Meads *et al.*[56] We have not carried out the calculations of Y, Θ_M, and $\langle u^2\rangle$ for lead as no experimental data are available for comparison purposes.

V. DISCUSSION AND CONCLUSION

We have studied the lattice vibrations and other thermal properties of six fcc metals by means of a simple scheme in which the interionic interactions of the metal ions are determined by the Morse potential, and the electron-ion interactions are determined by a screened Coulomb interaction. The ion-ion interaction (Morse potential) is a short-range interaction whereas the electron-ion interaction is long ranged. There are only four parameters in our model, yet the model gives an excellent agreement between the calculated and the experimental results for phonon dispersion relations, as well as the thermal properties of all the metals studied. The success of a lattice-dynamical model is judged by its ability to reproduce the experimental phonon dispersion relations. In that sense, the present model is a good one. The calculation of the thermal properties are the statistical properties which require a knowledge of a great many phonons in nonsymmetry directions. Thus agreement with these properties tests the validity of our model for the reproduction of phonons in the nonsymmetry directions. We are aware that very few measurements are available for phonon energies in the nonsymmetry directions, and until the time when such measurements are available, we can only compare our theoretical results with statistical properties.

We investigated the application of the Morse function in the lattice-dynamical studies of metals. We have adopted a new method here to derive D, α, and r_0 by considering the influence of conduction electrons. To the best of our knowledge, this is the first time such a study has been carried out. An interesting feature was observed, namely that the phonon dispersion relations were almost the same whether the interionic interactions were considered to the second-nearest neighbor or to twelfth-nearest neighbor. However, we found a marked difference between the first- and the second-nearest-neighbor interactions. This study is consistent with some of the earlier studies on lattice dynamics of fcc metals by Shukla and Closs,[57] Krebs,[28] and Bhatia.[58] While these authors utilize only the first and second derivatives of the interionic interactions as parameters (irrespective of the form of the interionic potential), we know that our interionic interactions are given by means of a Morse function.

Although the Morse function without electronic in-

teractions has been successfully applied to the study of numerous "static" lattice properties, including large-strain crystal deformations (see, e.g., the review article cited in Ref. 26) and crystal anharmonicity,[59] evidently it is important to include the electron gas in the description of lattice dynamics. To illustrate this importance, we have also computed phonon dispersion relations along the principal symmetry directions using the parameters D, α, and r_0 determined by Milstein[25] and Girifalco and Weizer.[13] We find that these parameters do not give a good description of the computed phonons, especially in the high-frequency region (see Figs. 1–6). Furthermore, a large departure is observed in the longitudinal frequencies along $[q00]$ and $[qq0]$ directions.

Recently, there has been great theoretical interest to guess a form of an interatomic potential which reproduces the experimental phonons. Some important work in this field has been done by, for example, Schneider and Stoll,[60] Moriarty,[61] Dagens *et al.*,[62] Brosens *et al.*,[63] Van Heughten,[64] and Esterling and Swaroop.[65] It is interesting to note that some of the workers utilize a least-squares fit by using as many as 5–10 parameters to obtain the form of their potential. However, this approach has limited physical justification. The model that we present in this paper is based on the Morse function, which has been successfully used in the study of a wide variety of properties in solid-state physics. The present study further enhances the field of study as well as the capabilities of the Morse function to successfully explain the lattice vibrations and the related properties in cubic metals, fcc being the specific case. There is, however, a limitation on the application of this approach. As shown by Milstein,[25] the ratio

$$[PG(2\alpha a)-QG(\alpha a)]/[PH(2\alpha a)-QH(\alpha a)] ,$$

and hence C_{11}^i/C_{12}^i [see Eqs. (34) and (35)], does not exceed approximately 1.36 for bcc crystals and is approximately bounded by $1.14<C_{11}^i/C_{12}^i<2.0$ for fcc crystals. This is a property of the Morse function and is independent of the particular form of electron-gas interaction. Thus the present method could not be applied to metals for which

$$C_{11}^i/C_{12}^i=(C_{11}-C_{12}+C_{44})/C_{44}$$

is outside of the indicated ranges (i.e., the experimental values of elastic moduli C_{ij} determine whether the present method can be employed). In practice, we could study only six of the dozen or so fcc metals for which the experimental C_{ij} were available. In the case of bcc metals, only potassium fulfills this requirement. We are presently calculating the vibrational properties of potassium by the scheme described in this paper. These results will be reported elsewhere.

ACKNOWLEDGMENT

One of us (F.M.) gratefully acknowledges the support of National Science Foundation Grant No. DMR-81-06022.

*Permanent address: Instituto de Fisica, Universidade Estadual de Campinas, Caixa Postal 1170, 13100 Campinas, São Paulo, Brazil.

[1]H. Eichler and M. Pegel, Phys. Status Solidi 35, 333 (1969).
[2]H. Diener, R. Heinrich, and W. Schellenberger, Phys. Status Solidi B 44, 403 (1971).
[3]V. Vitek, C. R. Perrin, and D. K. Bowen, Philos. Mag. 21, 1049 (1970).
[4]P. C. Gehlen, A. R. Rosenfield, and G. T. Hahn, J. Appl. Phys. 39, 5246 (1968).
[5]R. Chang, Philos. Mag. 16, 1021 (1967).
[6]R. M. J. Cotterill and M. Doyama, Phys. Rev. 145, 465 (1966).
[7]M. Doyama and R. M. J. Cotterill, Phys. Rev. 137, A994 (1965).
[8]R. A. Johnson, Phys. Rev. 134, A1329 (1964).
[9]L. A. Girifalco and V. G. Weizer, J. Phys. Chem. Solids 12, 260 (1960).
[10]W. D. Wilson and C. L. Bisson, Phys. Rev. B 3, 3979 (1971).
[11]A. Anderman and W. G. Gehman, Phys. Status Solidi 30, 283 (1968).
[12]R. Furth, Proc. R. Soc. London 183, 87 (1944).
[13]L. A. Girifalco and V. G. Weizer, Phys. Rev. 114, 687 (1959).
[14]D. H. Tsai and C. W. Beckett, J. Geophys. Res. 71, 2601 (1966).
[15]M. Drechsler and J. F. Nicholas, J. Phys. Chem. Solids 28, 2597 (1967).
[16]R. C. Lincoln, K. M. Koliwad, and P. B. Ghate, Phys. Rev. 157, 463 (1967).
[17]H. J. Leamy, Acta Metall. 15, 1839 (1967).
[18]J. Vail, Can. J. Phys. 45, 2661 (1967).
[19]M. Drechsler and J. F. Nicholas, J. Phys. Chem. Solids 28, 1609 (1967).
[20]F. O. Goodman, Phys. Rev. 164, 1113 (1967).
[21]R. Chang, in *Proceedings of the Second International Conference on Fracture* (Brighton, 1969) (unpublished).
[22]M. Born and R. Furth, Proc. Cambridge Philos. Soc. 36, 454 (1940).
[23]F. Milstein, Phys. Rev. B 3, 1130 (1971); F. Milstein and B. Farber, Philos. Mag. A 42, 19 (1980).
[24]H. O. Pamuk and T. Halicioglu, Phys. Status Solidi A 37, 695 (1976).
[25]F. Milstein, Phys. Rev. B 2, 512 (1970); J. Appl. Phys. 44, 3825 (1973).
[26]As shown by R. Hill and F. Milstein [Phys. Rev. B 15, 3087 (1977)], the Green moduli C_{ij} at nonzero pressure P are related to the shear moduli μ and μ' by $\lambda C_{44}=\mu'+P$ and $\frac{1}{2}\lambda(C_{11}-C_{12})=\mu+P$, where λ is the all-round stretch. Rigorously, $\mu=\mu^i$ and $\mu'-\mu'^i$ (instead of $C_{11}-C_{12}=C_{11}^i-C_{12}^i$ and $C_{44}=C_{44}^i$), since the electronic contributions are volume dependent only, and therefore do not contribute to the shear moduli. Here μ and μ' are the shear moduli of the crystal at $P=0$ (when both the ionic and electronic contributions are included) and μ^i and μ'^i are the shear moduli at the same atomic volume when only the ionic contributions are included. The topic of elastic moduli of cubic crystals under pressure is dealt with thoroughly by F. Milstein and R. Hill [J. Mech. Phys. Solids 25, 457 (1977); 26, 213 (1978); 27, 255 (1979)] and in a review article by Milstein [in *Mechanics of*

Solids, edited by H. G. Hopkins and M. J. Sewell (Pergamon, Oxford, 1982), pp. 417-452].
[27]N. P. Gupta and R. K. Gupta, Can. J. Phys. 47, 617 (1969).
[28]K. Krebs, Phys. Rev. 138, A143 (1964).
[29]E. C. Svensson, B. N. Brockhouse, and J. M. Rose, Phys. Rev. 155, 619 (1967).
[30]D. L. Martin, Can. J. Phys. 38, 17 (1960).
[31]E. A. Owen and R. W. Williams, Proc. R. Soc. London Ser. A 188, 509 (1947).
[32]P. A. Flinn, G. McManus, and J. A. Rayne, Phys. Rev. 123, 809 (1961).
[33]D. R. Chipman and A. Paskini, J. Appl. Phys. 30, 1992 (1959).
[34]W. Drexel, W. Glaser, and F. Gompf, Phys. Lett. 28A, 531 (1959).
[35]W. A. Kamitakahara and B. N. Brockhouse, Phys. Lett. 29A, 639 (1969).
[36]P. F. Meads, W. R. Forsythe, and W. F. Giauque, J. Am. Chem. Soc. 63, 1902 (1941).
[37]F. E. Hoare and B. Yates, Proc. R. Soc. London, Ser. A 240, 42 (1957).
[38]J. Boskovits, M. Roilos, A. Theodossion, and K. Alexopoulos, Acta Crystallogr. 11, 845 (1958).
[39]R. Andriessen, Physica (The Hague) 2, 417 (1935).
[40]J. Spreadborough and J. W. Christian, Proc. Phys. Soc. London 74, 609 (1959).
[41]M. Simareká, Czech. J. Phys. B 12, 658 (1962).
[42]J. W. Lynn, H. G. Smith, and R. M. Nicklow, Phys. Rev. B 8, 3494 (1973).
[43]W. S. Gorek, M. P. Garfunkel, C. B. Satterthwaite, and A. Wexter, Phys. Rev. 98, 1599 (1955).
[44]D. L. Martin, Phys. Rev. 141, 576 (1966).
[45]T. H. Geballe and W. F. Giauque, J. Am. Chem. Soc. 74, 2368 (1952).
[46]K. C. Turberfield, Atomic Energy Research Establishment (Harwell) Report No. PR/SSP-4, 13 (unpublished).
[47]M. W. Stringfellow and B. H. Torrie, Atomic Energy Research Establishment Report No. PR/SSP-5, 18 (unpublished).
[48]R. J. Birgeneau, J. Cordes, G. Dolling, and A. D. B. Woods, Phys. Rev. 136, A1387 (1964).
[49]R. H. Busey and W. F. Giauque, J. Am. Chem. Soc. 74, 3157 (1952).
[50]R. H. Wilson, E. F. Spelton, and J. L. Katz, Acta. Crystallogr. 21, 635 (1966).
[51]A. P. Miller and B. N. Brockhouse, Phys. Rev. Lett. 20, 798 (1968).
[52]G. J. Pickard and F. E. Simon, Proc. Phys. Soc. London 61, 1 (1968).
[53]K. Clusius and L. Schachinger, Z. Naturforsch. Teil A 2, 90 (1947).
[54]B. N. Brockhouse, T. Arase, G. Gaglioto, K. R. Roa, and A. D. B. Woods, Phys. Rev. 128, 1099 (1962).
[55]B. J. C. Van der Hoeven, Jr. and P. H. Keesom, Phys. Rev. 137, A103 (1965).
[56]P. F. Meads, W. R. Forsythe, and W. F. Giauque, J. Am. Chem. Soc. 63, 1902 (1941).
[57]M. M. Shukla and H. Closs, J. Phys. F 3, L1 (1973).
[58]A. B. Bhatia, Phys. Rev. 97, 363 (1955).
[59]F. Milstein and D. Rasky, Philos. Mag. A 45, 49 (1982).
[60]T. Schneider and E. Stoll, Phys. Kondens. Mater. 5, 331 (1966).
[61]J. A. Moriarty, Phys. Rev. B 10, 3075 (1974).
[62]L. Dagens, M. Rasolt, and R. Taylor, Phys. Rev. B 11, 2726 (1975).
[63]F. Brosens, J. Cornelis, D. C. Wallace, and J. T. Devreese, Phys. Status Solidi B 81, 557 (1977).
[64]W. F. W. M. Van Heughten, Phys. Status Solidi B 82, 501 (1977).
[65]D. M. Esterling and A. Swaroop, Phys. Status Solidi B 97, 101 (1980).